Optics Communications 285 (2012) 269–273

Contents lists available at SciVerse ScienceDirect

Optics Communications

journal homepage: www.elsevier.com/locate/optcom

Pressure and temperature characterization of two interferometric configurations based on suspended-core fibers

S.H. Aref [a,b,c], M.I. Zibaii [c], M. Kheiri [c], H. Porbeyram [c], H. Latifi [c,*], F.M. Araújo [a], L.A. Ferreira [a], J.L. Santos [a,d], J. Kobelke [e], K. Schuster [e], O. Frazão [a]

[a] INESC Porto – Instituto de Engenharia de Sistemas e Computadores do Porto, Rua do Campo Alegre, 687, 4169-007 Porto, Portugal
[b] Department of Physics, University of Qom, 3716146611 Qom, Iran
[c] Laser and Plasma Research Institute, Shahid Beheshti University, Tehran, Iran
[d] Departamento de Física da Faculdade de Ciências da Universidade do Porto, Rua do Campo Alegre, 687, 4169-007 Porto, Portugal
[e] IPHT – Institute of Photonic Technology, D-07745 Jena, Germany

ARTICLE INFO

Article history:
Received 24 February 2011
Received in revised form 14 September 2011
Accepted 18 September 2011
Available online 1 October 2011

Keywords:
Optical fiber sensors
Microstructured fiber
Sagnac and Fabry–Pérot interferometers

ABSTRACT

In this work, two all-fiber interferometric configurations based on suspended core fibers (SCF) are investigated. A Fabry–Pérot cavity (FPC) made of SCF spliced in-between segments of single-mode and hollow-core fiber is proposed. The interferometric signals are generated by the refractive-index mismatches between the two fibers in the splice region and at the end of the suspended-core fiber. An alternative sensing head configuration formed by the insertion of a length of SCF as a birefringence element in a Sagnac loop interferometer is also demonstrated. In this structure, the interferometric signals are generated by interfering two counter propagating beams with different polarization states which propagate through a length of SCF as a birefringence element. The sensitivity to pressure and temperature was determined for both configurations. The results show that the pressure sensitivities are -4.68×10^{-5} nm/psi and 0.032 nm/psi for FPC and Sagnac loop interferometers, respectively. The temperature sensitivity of both structures has been obtained and the results have been discussed.

1. Introduction

Many optical fiber sensing structures have been demonstrated in the past for pressure and temperature measurement. The fiber pressure sensors based on fiber Bragg grating [1, 2], Fabry–Pérot interferometer [3, 4], birefringence effects [5], and polarimetric Fabry–Pérot fiber laser sensor [6] have been studied in detail. The fiber Fabry–Pérot based on diaphragm deflection with low sensitivity to temperature has been suggested for high pressure measurement [3]. Side-hole fiber as a birefringence element has also been theoretically and experimentally investigated by Colwes et al. as a pressure sensor [5]. On the other hand, development of sensors based on microstructure optical fibers (MOFs) has been a recent and active research topic in the context of fiber optic sensing. Several types of MOF-based sensors, such as those based on suspended core fibers [7], index-guiding fibers [8] or photonic band gap fibers [9] have been reported. Particularly relevant is the application of these fibers for gas sensing in face of the large overlap of the optical field with the measurement volume [9], but other measurands have also been considered, for example bend and shape [10], strain and temperature [11], as well as hydrostatic pressure [12]. The suspended-core fiber structure was first proposed by Monro et al. [7], and one of the initial envisaged applications was gas sensing. Thanks to the noticeable evanescence wave propagated through the several holes around the small solid core, an evanescent device has been demonstrated for the sensing of acetylene gas at near-IR wavelengths [13]. Based on the same optical phenomenon, refractometric applications have also been considered, as is illustrated in a recent work in which a fiber Bragg grating, photo written in a suspended Ge-doped silica core, was used to measure the refractive index of liquids [14]. Macpherson et al. [15] presented the finite element analysis and experimentally pressure test of a Fabry–Perot sensor based on a microstructured optical fiber with a cross section similar to the suspended core fiber. The results demonstrated that the microstructured fiber has enhanced pressure sensitivity due to a high air-fraction in the cladding. Recently, Fu et al. [16] experimentally demonstrated the pressure response of a Sagnac loop incorporating a length of polarization--maintaining photonic crystal fiber, namely PM-PCF. Also, Frazão et al. [17] characterized the strain and temperature response of a Sagnac interferometric sensor with a four-hole suspended-core fiber. Also, a fiber-optic Fabry–Pérot sensing structure based on the utilization of 3-hole and 4-hole suspended-core fibers was presented by Frazão et al. [18].

In this work, the pressure sensitivity of two interferometric setups based on suspended core fibers is studied and their temperature response measured to assess the pressure/temperature cross sensitivity. The spectral response of the interferometers is determined by using

* Corresponding author. Tel.: +98 21 2990 2675.
E-mail address: latifi@cc.sbu.ac.ir (H. Latifi).

0030-4018/$ – see front matter © 2011 Elsevier B.V. All rights reserved.
doi:10.1016/j.optcom.2011.09.040

an optical spectrum analyzer and the measurand induced shift of this response obtained to characterize the measurand sensitivity.

2. Fiber sensor structures

Two sensing interferometric configurations based on suspended-core fiber were fabricated. One is a Fabry–Pérot Cavity and the second one a Sagnac loop incorporating a length of suspended-core fiber. The suspended-core fiber was made of pure silica at the Institute of Photonic Technology (IPHT, Jena, Germany). The four air-holes with about 43 μm diameter surrounded a silica core with about 5 μm in diameter. A schematic of the FPC as a sensing head and the cross section microscopic image of SCF have been presented in Fig. 1 (a). Fig. 1 (b) illustrates schematically the SCF based Sagnac interferometer.

The first interferometric configuration proposed for pressure measurement is based on a Fabry–Pérot cavity (FPC) and consists in a length of 5.2 mm SCF (cavity length). In the input side this fiber was spliced to the SMF-28. The SCF is made of a single material (pure silica) and the mismatch between the effective refractive indexes of the guided light in the SMF28 and SCF fibers provides the first Fresnel reflection of the Fabry–Pérot cavity. The second one was obtained by splicing a length (3 cm) of HCF to the end of SCF, originating a Fresnel reflection with the magnitude of an interface silica–air, enhancing the strength of the interferometric signal (the unbalance of the Fresnel reflections implies also a reduction of the interferometric fringe visibility, which means a reduction of the interferometric signal; however, the visibility reduction is a weak function of the this unbalance, having a smaller effect than the positive one associated with a higher signal-to-noise ratio derived from having higher levels of optical power in the interferometer). The splicing of the SCF with the SMF-28 has been done with a standard fusion splice machine in manual operation, resulting in a splice loss of ~5 dB. This value is mainly determined by the fact that the core of the SCF is slightly elliptical owing to the hole asymmetry originated during the fabrication process.

The end of HCF was closed by collapsing the fiber by inducing a high electric discharge. By this way the liquid cannot penetrate into the HCF and holes of SCF. The channeled spectrum of the FPC is shown in Fig. 2 (a). As can be observed, after splicing the visibility and phase of the interferometer are changed. These variations are expected due to changes introduced by the electric arc at the end of the suspended-core fiber. We should emphasize that the phase change is in major part due to the impact of electric arc in length and refractive index of the fiber.

The second interferometric sensor based on SCF proposed for pressure measurement is based on a Sagnac loop incorporating a length of this fiber (~ 89 cm), spliced between two single mode fibers (SMF-28). In the Sagnac interferometer the birefringence of the SCF gives origin to a channeled spectrum that shifts with the variation of the external pressure. This is shown in Fig. 2 (b), where the spectral response of the Sagnac loop interferometer and the corresponding shift of the interferometric pattern are depicted when the sensing head was pressurized at three different pressure values. From this data, the group modal birefringence (β) of the SCF was obtained using the equation $\beta = \lambda^2/L\Delta\lambda$, where λ is the operation wavelength (1550 nm), and $\Delta\lambda$ and L are the spectral wavelength period of the interferometric fringe pattern and the length of the SCF, respectively. Using the mentioned parameters and also the value of spectral wavelength period ($\Delta\lambda = 71$ nm) it was found that $\beta \approx 3.8 \times 10^{-5}$.

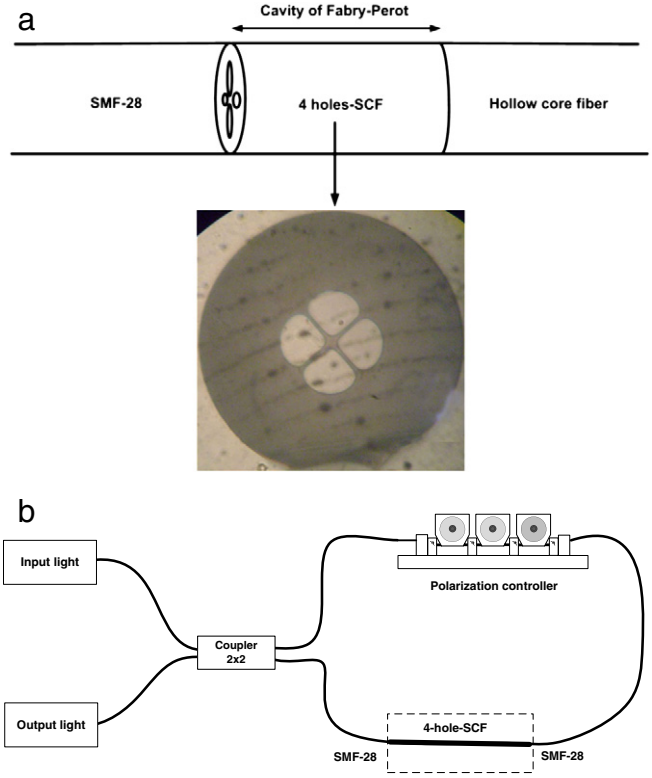

Fig. 1. (a) A schematic of the FPC as a sensing head and the cross section microscopic image of SCF. (b) A schematic of the SCF based Sagnac interferometer.

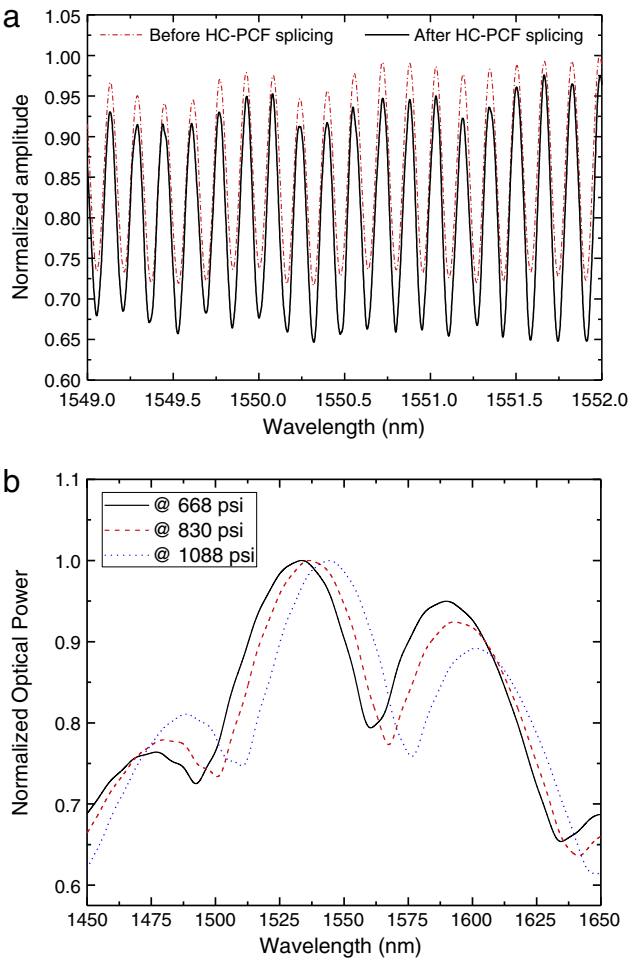

Fig. 2. (a) Spectral response of the FPC with a 4-hole SCF before and after the splicing with a hollow-core fiber. (b) Spectral response of the Sagnac interferometer with a length of 4-hole SCF at three different pressures.

3. Experimental setup and results

To determine the pressure sensitivity of the FPC, it was placed inside a high pressure vessel and the SMF-28 was sealed to cap of a high pressure vessel and then hydrostatic pressure was applied. The vessel was pressurized by injection of the water by a high pressure unit. Fig. 3 shows the experimental setup. To illuminate the system a broadband optical source with a bandwidth of 70 nm and a central wavelength of 1550 nm was used. The FPC was interrogated in reflection via a 2×2 coupler and an Agilent 86142B OSA with a maximum resolution of 10 pm.

The SMF was bonded to form a sealed feed through on the high pressure vessel by using a two components adhesive. Pressure was applied in a range from 0 psi up to 4000 psi (in comparison to atmospheric pressure), measured using a high precision pressure gauge (±5 psi accuracy). The test was done at room temperature. Additionally, this sensing head was also characterized for temperature variation. In order to do that, it was placed in an oven where the temperature was set from room temperature up to 90 °C, with a variation lower than 0.1 °C. The pressure and temperature response of the sensor were obtained by registering the measurand induced shift of the cavity channeled spectrum. The results are shown in Fig. 4. In both situations, a linear variation is observed with slopes of -4.68×10^{-5} nm/psi and -0.011 nm/°C for pressure and temperature, respectively.

Fig. 5 illustrates the experimental setup for pressure characterization of the sensing head based on the Sagnac interferometer. It consists of an edge light emitting diode (ELED), an Agilent 86142B OSA and a Sagnac loop interferometer containing a length of 4-hole SCF and a polarization controller to optimize the interferometric fringes visibility. To apply hydrostatic pressure to the SCF, a length of fiber of the Sagnac loop containing the whole SCF was wrapped around a tube and placed inside the high pressure vessel. The vessel input/output fibers were sealed as indicated before.

The results obtained are shown in Fig. 6 where the shift of the channeled spectrum when the measurand changes is presented. For the case of pressure, a linear dependence is observed with a slope of ~0.032 nm/psi. The temperature characterization of the sensing head has been done at two distinct conditions, namely the SCF coated (suspended-core fiber length of ~89 cm) and uncoated (length of ~32 cm). For the uncoated case, the temperature sensitivity is residual as a consequence of the low temperature dependence of the

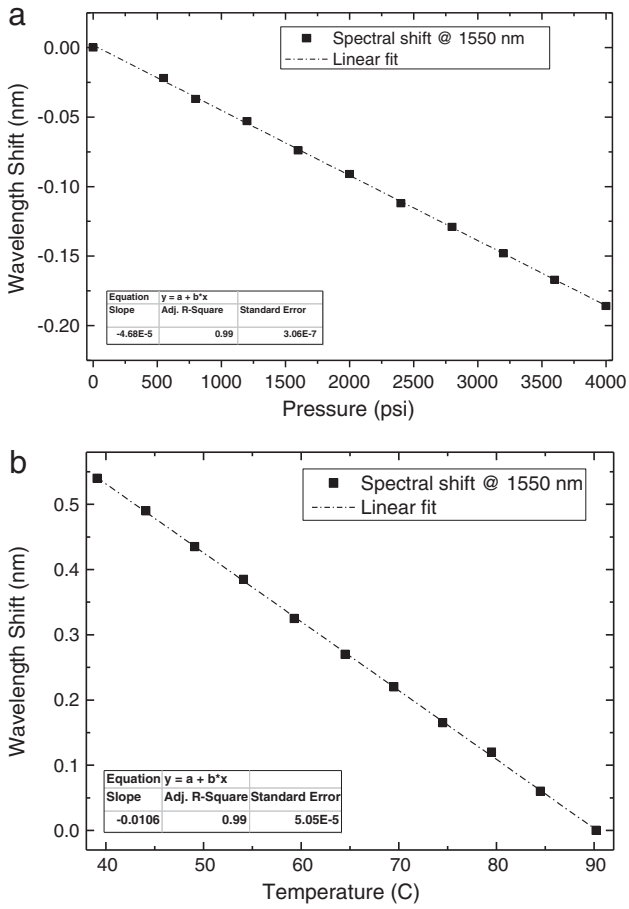

Fig. 4. Pressure and temperature responses of the SCF based Fabry–Perot interferometer.

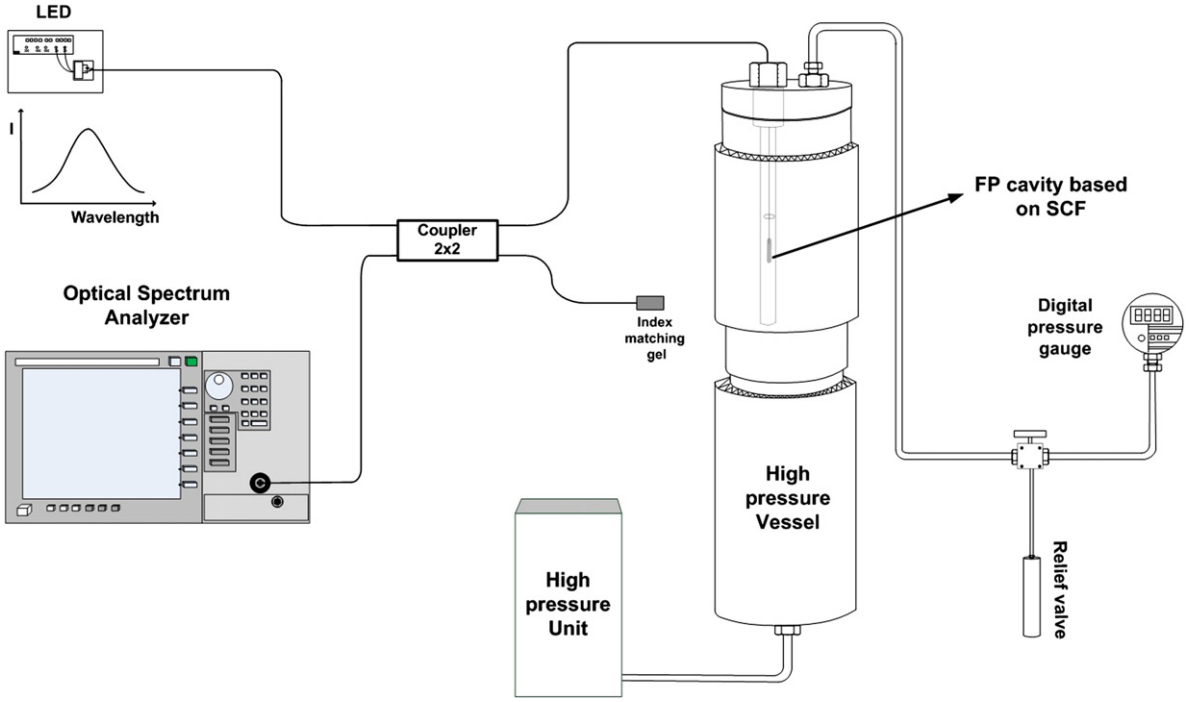

Fig. 3. Experimental setup for pressure characterization of the SCF based Fabry–Pérot interferometer.

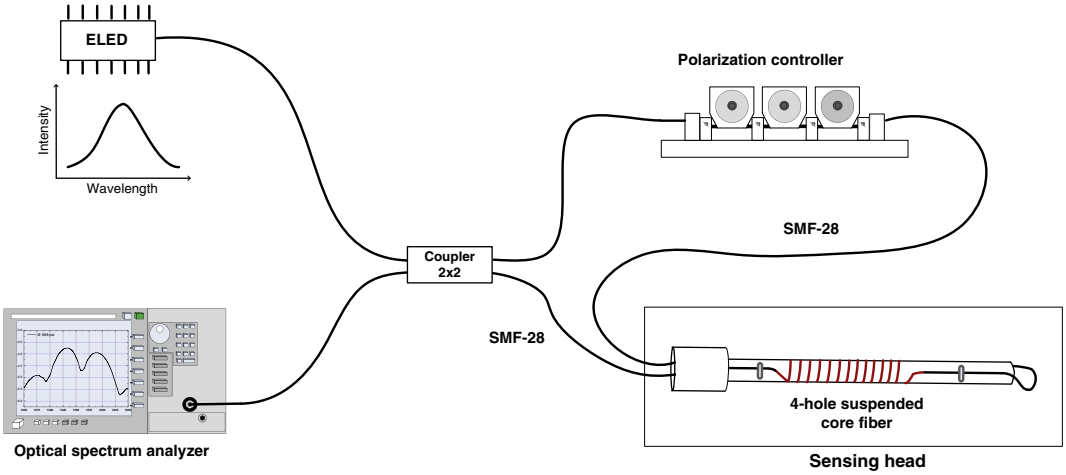

Fig. 5. Experimental setup for pressure characterization of the SCF based Sagnac interferometer.

SCF birefringence. This happens because this fiber is formed by pure silica, i.e., has no doping, the birefringence is only appearing due to the geometrical asymmetry of the core. The small temperature cross-sensitivity is a favorable characteristic of this structure for pressure measurement compared with the one based on the FPC. On the other hand, the condition with coated fiber also shows negligible temperature sensitivity up to the temperature of ~60 °C, where a kind of "phase transition" appears, probably due to the release of the coating tension on the silica associated with the softening of the coating. , we can compare the normalized pressure sensitivity of both interferometric structures with experimentally pressure sensitivity of similar structures which has been reported in literature. MacPherson et al. [15] has reported the pressure sensitivity of FPC based on a similar 3-hole SCF which core is approximately 5 μm in diameter and is supported by three strands of glass 24 μm × 2 μm. The pressure sensitivities of FPC based on 3-hole SCF and SMF-28 were found to be 7.86 rad/bar/m 2.37 rad/bar/m, respectively. Also Fu et al. [16] have obtained the pressure sensitivity of a PM-PCF based Sagnac loop interferometer sensor. The sensitivity of the pressure sensor was measured to be 3.24 nm/Mpa at 1509.8 nm. The normalized pressure sensitivity of the results for pressure sensitivity in 1/psi unit for FPCs based on three different fibers, namely 4-hole SCF and 3-hole SCF and SMF-28, are presented in Table 1. It should be noticed that the conversion can be facilitated using the relation $d\phi = (4\pi nL/\lambda^2)d\lambda$, where L is the cavity length, n is the effective refractive index of the guided mode and λ is the operating wavelength (around 1550 nm). We obtained the conversion factor using the refractive index 1.46, at 1550 nm for pure silica. Also, the table shows the normalized pressure sensitivity for SCF and PM-PCF based Sagnac loop interferometer. The sign of pressure sensitivity in FPC and Sagnac based sensors is opposite. For the FPC based sensor the pressure sensitivity is the sum of axial and strain-optic effects resulting into a negative value [19]. On the other hand, for the Sagnac based sensor the sign of pressure sensitivity is determined only by the birefringence–pressure coefficient of the 4-hole SCF [20], which in this case is positive.

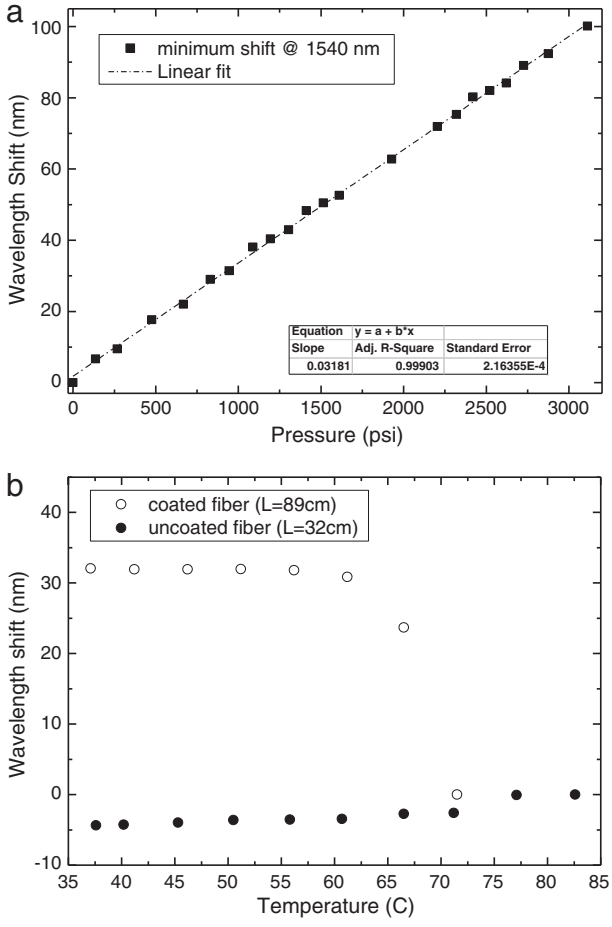

Fig. 6. Experimental setup for pressure characterization of the SCF based Sagnac interferometer.

The results in Table 1 underline a pressure sensitivity enhancement of ≈2.2 for FPC sensor in comparison to SMF; also the result for 4-hole SCF based Sagnac interferometer shows the highest sensitivity.

4. Conclusion

In this work two sensing structures based on pure silica suspended-core fibers were proposed and characterized for pressure and

Table 1
Pressure and temperature sensitivity of FPC with different optical fiber.

Sensor based FPC	4-hole SCF	3-hole SCF [15]	SMF-28 [15]
Pressure sensitivity	-4.68×10^{-5} nm/psi	−7.86 rad/bar/m	−2.37 rad/bar/m
Normalized pressure sensitivity (1/psi)	-0.030×10^{-6}	-0.046×10^{-6}	-0.014×10^{-6}
Sensor based Sagnac interferometer		**4-hole SCF**	**PM-PCF [16]**
Pressure sensitivity		0.03 nm/psi	3.24 nm/MPa
Normalized pressure sensitivity (1/psi)		20.6×10^{-6}	14.8×10^{-6}

temperature measurement. One is a Fabry–Pérot configuration that shows sensitivities of -4.68×10^{-5} nm/psi and -0.0106 nm/°C for pressure and temperature, respectively. The second structure investigated is a Sagnac interferometer incorporating a length of suspended-core fiber as a birefringence element. In this case, a pressure sensitivity of 0.032 nm/psi was obtained . The temperature sensitivity of this sensing head depends on the presence or not of fiber coating, being residual thus essentially eliminating the temperature cross-sensitivity problem. The small temperature cross-sensitivity is a favorable characteristic of this structure for pressure measurement compared with the one based on the Fabry–Pérot cavity, which anyway has its own advantages namely the small dimensions and also its operation independent of the polarization.

Acknowledgment

This work was performed in the framework of European Program COST, Action 299 “Optical Fibers for New Challenges Facing the Information Society”.

References

[1] W.T. Zhang, F. Li, Y.L. Liu, L.H. Liu, IEEE Photonics Technology Letters 19 (2007) 1553.
[2] J. Yanga, Y. Zhaoa, B.J. Pengb, X. Wanb, Sensors and Actuators A 118 (2005) 254.
[3] J. Xu, G. Pickrell, X. Wang, W. Peng, K. Cooper, A. Wang, IEEE Photonics Technology Letters 17 (2005) 870.
[4] S.H. Aref, M.I. Zibaii, H. Latifi, Measurement Science and Technology 20 (2009) 034009.
[5] J.R. Clowes, S. Syngellakis, M.N. Zervas, IEEE Photonics Technology Letters 10 (1998) 857.
[6] K. Bohnert, A. Frank, E. Rochat, K. Haroud, H. Brandle, Applied Optics 43 (2004) 41.
[7] T.M. Monro, W. Belardi, K. Furusawa, J.C. Baggett, N.G.R. Broderick, D.J. Richardson, Measurement Science and Technology 12 (2001) 854.
[8] Y.L. Hoo, W. Jin, C. Shi, H.L. Ho, D.N. Wang, S.C. Ruan, Applied Optics 42 (2003) 3509.
[9] R. Thapa, K. Knabe, K.L. Corwin, B.R. Washburn, Optics Express 14 (2006) 9576.
[10] W.N. MacPherson, M.J. Gander, R. McBride, J.D.C. Jones, P.M. Blanchard, J.G. Burnett, A.H. Greenaway, B. Mangan, T.A. Birks, J.C. Knight, P.St.J. Russell, Optics Communication 193 (2001) 97.
[11] C. Zhao, L. Xiao, J. Ju, M.S. Demokan, W. Jin, Journal of Lightwave Technology 26 (2008) 220.
[12] W.N. MacPherson, E.J. Rigg, J.D.C. Jones, V.V. Ravi, K. Kumar, J.C. Knight, P.St.J. Russell, Journal of Lightwave Technology 23 (2005) 1227.
[13] A.S. Webb, F. Poletti, D.J. Richardson, J.K. Sahu, Optical Engineering 46 (2007) 010503-1.
[14] M.C.P. Huy, G. Laffont, V. Dewynter, P. Ferdinand, P. Roy, J.L. Auguste, D. Pagnoux, W. Blanc, B. Dussardier, Optics Letters 32 (2007) 2390.
[15] W.N. MacPherson, E.J. Rigg, J.D.C. Jones, V.V. Ravi Kanth Kumar, J.C. Knight, P.St.J. Russell, Journal of Lightwave Technology 23 (2005) 1227.
[16] H.Y. Fu, C. Wu, M.L.V. Tse, L. Zhang, Kei-Chun D. Cheng, H.Y. Tam, Bai-Ou Guan, C. Lu, Applied Optics 49 (2010) 2639.
[17] O. Frazão, J.M. Baptista, J.L. Santos, J. Kobelke, K. Schuster, Electronics Letters 44 (2008) 1455.
[18] O. Frazão, S.H. Aref, J.M. Baptista, J.L. Santos, H. Latifi, F. Farahi, J. Kobelke, K. Schuster, IEEE Photonics Technology Letters 21 (2009) 1229.
[19] G.B. Hocker, Applied Optics 19 (1979) 1445.
[20] H.Y. Fu, H.Y. Tam, Li-Yang Shao, Xinyong Dong, P.K.A. Wai, C. Lu, Sunil K. Khijwania, Applied Optics 47 (2008) 2835.